A state observer for the Virgo inverted pendulum

T. Accadia,[1] F. Acernese,[2,3] P. Astone,[4] G. Ballardin,[5] F. Barone,[2,3] M. Barsuglia,[6] A. Basti,[7,8] Th. S. Bauer,[9] M. Bebronne,[1] M. G. Beker,[9] A. Belletoile,[1] M. Bitossi,[7] M. A. Bizouard,[10] M. Blom,[9] F. Bondu,[11] L. Bonelli,[7,8] R. Bonnand,[12] V. Boschi,[7,a)] L. Bosi,[13] B. Bouhou,[6] S. Braccini,[7] C. Bradaschia,[7] M. Branchesi,[14,15] T. Briant,[16] A. Brillet,[17] V. Brisson,[10] T. Bulik,[18] H. J. Bulten,[9,19] D. Buskulic,[1] C. Buy,[6] G. Cagnoli,[14] E. Calloni,[2,20] B. Canuel,[5] F. Carbognani,[5] F. Cavalier,[10] R. Cavalieri,[5] G. Cella,[7] E. Cesarini,[15] O. Chaibi,[17] E. Chassande-Mottin,[6] A. Chincarini,[21] A. Chiummo,[5] F. Cleva,[17] E. Coccia,[22,23] P.-F. Cohadon,[16] C. N. Colacino,[7,8] J. Colas,[5] A. Colla,[4,24] M. Colombini,[24] A. Conte,[4,24] A. Corsi,[4] J.-P. Coulon,[17] E. Cuoco,[5] S. D' Antonio,[22] V. Dattilo,[5] M. Davier,[10] R. Day,[5] R. De Rosa,[2,20] G. Debreczeni,[25] W. Del Pozzo,[9] M. del Prete,[26] L. Di Fiore,[2] A. Di Lieto,[7,8] M. Di Paolo Emilio,[22,27] A. Di Virgilio,[7] A. Dietz,[1] M. Drago,[26,28] G. Endrőczi,[25] V. Fafone,[22,23] I. Ferrante,[7,8] F. Fidecaro,[7,8] I. Fiori,[5] R. Flaminio,[12] L. A. Forte,[2] J.-D. Fournier,[17] J. Franc,[12] S. Frasca,[4,24] F. Frasconi,[7] M. Galimberti,[12] L. Gammaitoni,[13,29] F. Garufi,[2,20] M. E. Gáspár,[25] G. Gemme,[21] E. Genin,[5] A. Gennai,[7] A. Giazotto,[7] R. Gouaty,[1] M. Granata,[6] C. Greverie,[17] G. M. Guidi,[14,15] J.-F. Hayau,[11] A. Heidmann,[16] H. Heitmann,[17] P. Hello,[10] P. Jaranowski,[30] I. Kowalska,[18] A. Królak,[31,32] N. Leroy,[10] N. Letendre,[1] T. G. F. Li,[9] N. Liguori,[26,28] M. Lorenzini,[14] V. Loriette,[33] G. Losurdo,[14] E. Majorana,[4] I. Maksimovic,[33] N. Man,[17] M. Mantovani,[7,34] F. Marchesoni,[13] F. Marion,[1] J. Marque,[5] F. Martelli,[14,15] A. Masserot,[1] C. Michel,[12] L. Milano,[2,20] Y. Minenkov,[22] M. Mohan,[5] N. Morgado,[12] A. Morgia,[22,23] B. Mours,[1] L. Naticchioni,[4,24] F. Nocera,[5] G. Pagliaroli,[22,27] L. Palladino,[22,27] C. Palomba,[4] F. Paoletti,[5,7] M. Parisi,[2,20] A. Pasqualetti,[5] R. Passaquieti,[7,8] D. Passuello,[7] G. Persichetti,[2,20] F. Piergiovanni,[14,15] M. Pietka,[30] L. Pinard,[12] R. Poggiani,[7,8] M. Prato,[21] G. A. Prodi,[26,28] M. Punturo,[13] P. Puppo,[4] D. S. Rabeling,[9,19] I. Rácz,[25] P. Rapagnani,[4,24] V. Re,[22,23] T. Regimbau,[17] F. Ricci,[4,24] F. Robinet,[10] A. Rocchi,[22] L. Rolland,[1] R. Romano,[2,3] D. Rosińska,[35,36] P. Ruggi,[5] B. Sassolas,[12] D. Sentenac,[5] L. Sperandio,[22,23] R. Sturani,[14,15] B. Swinkels,[5] M. Tacca,[5] L. Taffarello,[37] A. Toncelli,[7,8] M. Tonelli,[7,8] O. Torre,[7,8] E. Tournefier,[1] F. Travasso,[13,29] G. Vajente,[7,8] J. F. J. van den Brand,[9,19] C. Van Den Broeck,[9] S. van der Putten,[9] M. Vasuth,[25] M. Vavoulidis,[10] G. Vedovato,[37] D. Verkindt,[1] F. Vetrano,[14,15] A. Viceré,[14,15] J.-Y. Vinet,[17] S. Vitale,[9] H. Vocca,[13] R. L. Ward,[6] M. Was,[10] M. Yvert,[1] A. Zadrożny,[32] and J.-P. Zendri[37]

[1]*Laboratoire d'Annecy-le-Vieux de Physique des Particules (LAPP), Université de Savoie, CNRS/IN2P3, F-74941 Annecy-Le-Vieux, France*
[2]*INFN, Sezione di Napoli, Complesso Universitario di Monte S.Angelo, I-80126 Napoli, Italy*
[3]*Università di Salerno, Fisciano, I-84084 Salerno, Italy*
[4]*INFN, Sezione di Roma, I-00185 Roma, Italy*
[5]*European Gravitational Observatory (EGO), I-56021 Cascina (PI), Italy*
[6]*Laboratoire AstroParticule et Cosmologie (APC) Université Paris Diderot, CNRS: IN2P3, CEA: DSM/IRFU, Observatoire de Paris, 10 rue A.Domon et L.Duquet, 75013 Paris, France*
[7]*INFN, Sezione di Pisa, I-56127 Pisa, Italy*
[8]*Università di Pisa, I-56127 Pisa, Italy*
[9]*Nikhef, Science Park, Amsterdam, The Netherlands*
[10]*LAL, Université Paris-Sud, IN2P3/CNRS, F-91898 Orsay, France*
[11]*Institut de Physique de Rennes, CNRS, Université de Rennes 1, 35042 Rennes, France*
[12]*Laboratoire des Matériaux Avancés (LMA), IN2P3/CNRS, F-69622 Villeurbanne, Lyon, France*
[13]*INFN, Sezione di Perugia, I-06123 Perugia, Italy*
[14]*INFN, Sezione di Firenze, I-50019 Sesto Fiorentino, Italy*
[15]*Università degli Studi di Urbino 'Carlo Bo', I-61029 Urbino, Italy*
[16]*Laboratoire Kastler Brossel, ENS, CNRS, UPMC, Université Pierre et Marie Curie, 4 Place Jussieu, F-75005 Paris, France*
[17]*Université Nice-Sophia-Antipolis, CNRS, Observatoire de la Côte d'Azur, F-06304 Nice, France*
[18]*Astronomical Observatory Warsaw University 00-478 Warsaw, Poland*
[19]*VU University Amsterdam, De Boelelaan 1081, 1081 HV Amsterdam, The Netherlands*
[20]*Università di Napoli 'Federico II' Complesso Universitario di Monte S.Angelo, I-80126 Napoli, Italy*

a)Author to whom correspondence should be addressed. Electronic mail: valerio.boschi@pi.infn.it.

[21]*INFN, Sezione di Genova, I-16146 Genova, Italy*
[22]*INFN, Sezione di Roma Tor Vergata, Italy*
[23]*Università di Roma Tor Vergata, I-00133 Roma, Italy*
[24]*Università 'La Sapienza', I-00185 Roma, Italy*
[25]*RMKI, H-1121 Budapest, Konkoly Thege Miklós út 29-33, Hungary*
[26]*Università di Trento, I-38050 Povo, Trento, Italy*
[27]*Università dell'Aquila, I-67100 L'Aquila, Italy*
[28]*INFN, Gruppo Collegato di Trento, I-38050 Povo, Trento, Italy*
[29]*Università di Perugia, I-06123 Perugia, Italy*
[30]*Białystok University 15-424 Białystok, Poland*
[31]*IM-PAN 00-956 Warsaw, Poland*
[32]*IPJ 05-400 Świerk-Otwock, Poland*
[33]*ESPCI, CNRS, F-75005 Paris, France*
[34]*Università di Siena, I-53100 Siena, Italy*
[35]*CAMK-PAN 00-716 Warsaw, Poland*
[36]*Institute of Astronomy 65-265 Zielona Góra, Poland*
[37]*INFN, Sezione di Padova, I-35131 Padova, Italy*

(Received 19 July 2011; accepted 22 August 2011; published online 26 September 2011)

We report an application of Kalman filtering to the inverted pendulum (IP) of the Virgo gravitational wave interferometer. Using subspace method system identification techniques, we calculated a linear mechanical model of Virgo IP from experimental transfer functions. We then developed a Kalman filter, based on the obtained state space representation, that estimates from open loop time domain data, the state variables of the system. This allows the observation (and eventually control) of every resonance mode of the IP mechanical structure independently. © *2011 American Institute of Physics*. [doi:10.1063/1.3637466]

I. INTRODUCTION

In order to detect gravitational waves (GW), the displacement of the test masses of modern interferometers, such as the Virgo experiment[1] and the Laser Interferometer Gravitational-wave Observatory (LIGO),[2] has to be reduced to the challenging level of 10^{-18} m/$\sqrt{\text{Hz}}$ in the 10 Hz–10 kHz detection band. For second generation detectors[3,4] the requirements are even more compelling. Since the seismic noise is the dominant low frequency noise source for terrestrial GW detectors, the performance, and reliability of seismic attenuation systems play a critical role.

Two approaches are typical in the design of seismic attenuation systems: active seismic attenuators heavily rely on control systems to reduce the ground motion, while passive isolators exploit the fundamental property that the response of a harmonic oscillator to seismic excitation is equivalent to a second-order low pass filter.

The Virgo superattenuator (SA) (Ref. 5) is an example of this latter approach and is capable of providing more than 10 orders of magnitude of seismic isolation in all six degrees of freedom above a few Hz. The SA mechanical structure, shown in Fig. 1, consists of three fundamental parts:

- the inverted pendulum (IP);
- the chain of seismic filters;
- the payload.

The IP (Ref. 6) is constituted of three 6 m-long hollow legs, each one connected to the ground through a flexible joint and supporting an interconnecting structure (the top ring) on its top. As shown in Fig. 2, the top ring, which is a mechanical support for an additional seismic filter, called filter 0, similar to those used in the chain, is equipped with a set of sensors and actuators, placed in a pinwheel configuration, that are used to actively damp the IP resonance modes. Two kinds of sensors, linear variable differential transformers (LVDTs) and high sensitivity accelerometers specifically designed for Virgo, and two sets of actuators, coil-magnets, and motor-springs, are used.

The chain of seismic filters is suspended from the filter 0 and is constituted by an 8 m-long set of five cylindrical passive filters, each one designed to reduce the seismic noise by 40 dB, starting from a few Hz, in both horizontal and vertical directions.

The payload is suspended from the last seismic filter of the chain and consists of the marionette (an anvil-shaped element, designed to steer the mirror), the reference mass, and the mirror.

The position and acceleration sensors on the top ring provide a signal proportional to a superposition of all SA mechanical resonances and the IP control is currently implemented by diagonalizing the sensor-actuator space in order to obtain three single-input single-output (SISO) systems. It would be useful to monitor and control each mode of the structure independently. For this reason we have developed a Kalman state observer based on a set of state-space models calculated from experimental data using system identification techniques. In Secs. II–III we will briefly discuss the theory involved and analyze the results obtained.

II. THEORY

A. IP linear model

In general, an n-degree of freedom mechanical system with viscous damping subject to holonomic constraints can be written in the small oscillation regime in the linear form:[7]

$$\mathbf{M}\ddot{\mathbf{q}}(t) + \Gamma\dot{\mathbf{q}}(t) + \mathbf{K}\mathbf{q}(t) = \mathbf{F}(t), \tag{1}$$

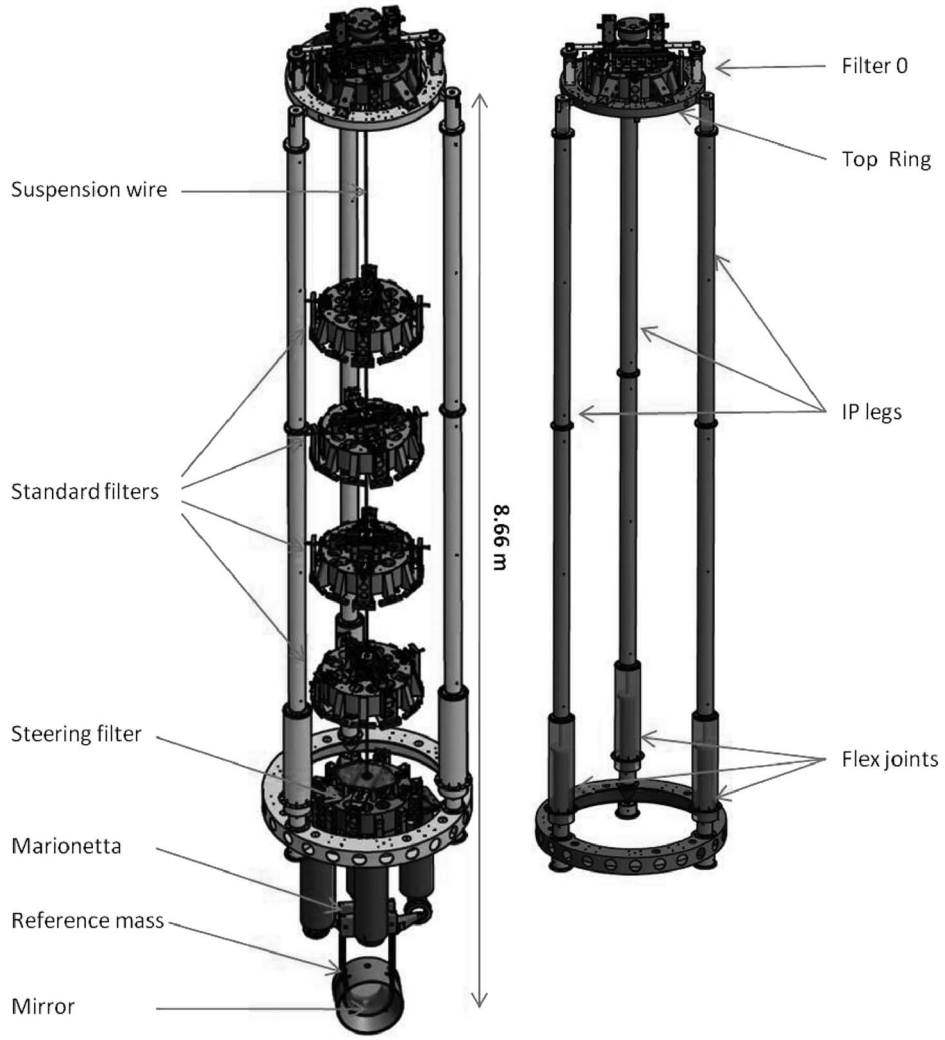

FIG. 1. Left: view from top of the VIRGO superattenuator. Right: detail of the VIRGO IP. We can distinguish, from top to bottom, the three legs of the inverted pendulum, the filter 0, the top ring, the passive filters 1 to 4, and the mirror control system. This last stage, constituted by the steering filter, the marionetta, and the reference mass, is dedicated to the control of the mirror position for frequencies $f > 100$ mHz.

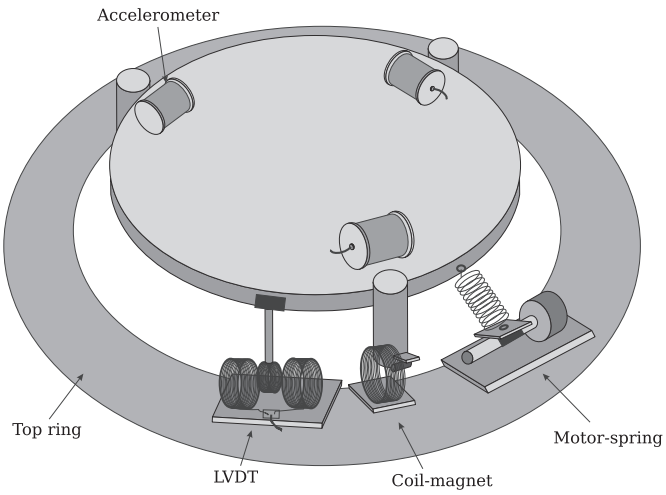

FIG. 2. View from top of the filter 0 mechanical support. The sensors and actuators are placed in a triangular configuration on the top ring, with the sensing axes tangent to the top table. For clarity only one LVDT and one set of actuators are shown.

where $\mathbf{q}(t) = [q_1(t), q_2(t), \ldots, q_n(t)]^T$ and $q_k(t)$ are the generalized coordinates, $\mathbf{M}$ is the mass matrix, Γ is the damping matrix, $\mathbf{K}$ is the stiffness matrix, and $\mathbf{F}(t)$ is a vector of generalized non-conservative forces. It can be easily shown that, introducing the state vector $\mathbf{x}(t) = [\mathbf{q}^T(t), \dot{\mathbf{q}}^T(t)]^T$, with dimension $N = 2n$, and the output vector $\mathbf{y}$, we can write Eq. (1) in state-space representation as

$$\dot{\mathbf{x}}(t) = \mathbf{A}\mathbf{x}(t) + \mathbf{B}\mathbf{F}(t), \tag{2}$$

$$\mathbf{y} = \mathbf{C}\mathbf{x}(t) + \mathbf{D}\mathbf{F}(t), \tag{3}$$

with

$$\mathbf{A} = \begin{pmatrix} \mathbf{0}_{n\times n} & \mathbf{I}_n \\ -\mathbf{M}^{-1}\mathbf{K} & -\mathbf{M}^{-1}\Gamma \end{pmatrix} \tag{4}$$

and

$$\mathbf{B} = \begin{pmatrix} \mathbf{0}_{n\times n} \\ \mathbf{M}^{-1} \end{pmatrix}. \tag{5}$$

We are now going to write a simple model of the IP control system.[8] In order to obtain a state-space representation of

the IP equations of motion, we assume the system in small oscillation regime and we approximate the dissipation mechanisms of the elastic elements with viscous damping. Moreover, since the frequencies of vertical, pitch, and roll IP modes are well above the unity gain bandwidth of the control loop, we consider only the Cartesian coordinates x, z, and θ_y where the x, z axes are aligned with the interferometer arms on the horizontal plane. Using generalized coordinates, we can therefore define the state vector of the IP control system as

$$\xi = (x, z, \theta_y, \dot{x}, \dot{z}, \dot{\theta}_y)^T. \tag{6}$$

Considering the coil currents as the system input vector $\mathbf{u}_A$ and the accelerometer signals as the output $\mathbf{y}_A$, we can write the IP equations of motion in the form

$$\dot{\xi} = \mathbf{A}_A \xi + \mathbf{B}_A \mathbf{u}_A + \mathbf{w}_A, \tag{7}$$

$$\mathbf{y}_A = \mathbf{S}_A \dot{\xi} + \mathbf{S}_T \xi + \mathbf{v}_A, \tag{8}$$

where $\mathbf{S}_A\dot{\xi}$ represents the IP center of mass acceleration projected along the accelerometers sensibility axis and $\mathbf{S}_T\xi$ is the top table tilt with respect to the horizontal direction. The vectors $\mathbf{w}_A$ and $\mathbf{v}_A$ represent the process and measurement noise, respectively. In a similar way, using the IP position measurements, provided by the LVDTs, as the system output $\mathbf{y}_L$, we have

$$\dot{\xi} = \mathbf{A}_L \xi + \mathbf{B}_L \mathbf{u}_L + \mathbf{w}_L, \tag{9}$$

$$\mathbf{y}_L = \mathbf{S}_L \dot{\xi} + \mathbf{v}_L. \tag{10}$$

Substituting Eqs. (7) into (8) and (9) into (10), we can rewrite both models in the standard form:

$$\dot{\xi} = \mathfrak{A}\xi + \mathfrak{B}\mathbf{u} + \mathbf{w}, \tag{11}$$

$$\mathbf{y} = \mathfrak{C}\xi + \mathfrak{D}\mathbf{u} + \mathbf{v}, \tag{12}$$

with $\mathfrak{A} = \mathbf{A}_A$, $\mathfrak{B} = \mathbf{B}_A$, $\mathfrak{C} = \mathbf{S}_A\mathbf{A}_A + \mathbf{S}_T$, $\mathfrak{D} = \mathbf{S}_A\mathbf{B}_A$, and $\mathbf{u} = \mathbf{u}_A, \mathbf{y} = \mathbf{y}_A, \mathbf{w} = \mathbf{w}_A, \mathbf{v} = \mathbf{v}_A + \mathbf{S}_A\mathbf{w}_A$ for the accelerometers model and $\mathfrak{A} = \mathbf{A}_L$, $\mathfrak{B} = \mathbf{B}_L$, $\mathfrak{C} = \mathbf{S}_L\mathbf{A}_L$, $\mathfrak{D} = \mathbf{S}_L\mathbf{B}_L$, and $\mathbf{u} = \mathbf{u}_L, \mathbf{y} = \mathbf{y}_L, \mathbf{w} = \mathbf{w}_L, \mathbf{v} = \mathbf{v}_L + \mathbf{S}_L\mathbf{w}_L$ for the LVDTs model.

B. System identification

The matrices of Eqs. (11) and (12) can be obtained from experimental data using subspace system identification. This technique allows to estimate a state-space representation of a given order N from the observed data of a multiple-input multiple-output (MIMO) system in the time domain. In particular, we used the MATLAB® system identification toolbox `n4sid` command,[9] that is a numerical implementation of the Overschee and Moore subspace identification method.[10]

The estimated state-space representations are, in general, not written in form (4). For this reason we scaled the models, in order to reduce their numerical range and sensitivity, and transformed them in modal representation, a canonic form in which the real eigenvalues of the **A** matrix appear on its diagonal and the complex conjugate eigenvalues appear in 2×2 blocks on its diagonal. This transformation is always possible if, as in our case,[11] the eigenvalues of **A** are all distinct. For a system with k real eigenvalues $\lambda_1, \ldots, \lambda_k$ and s complex eigenvalues $\sigma_1 \pm i\omega_1, \ldots, \sigma_s \pm i\omega_s$, with $k + s = N$, we have

$$\mathbf{A}_m = \begin{pmatrix} \lambda_1 & & & & & & \\ & \sigma_1 & \omega_1 & & & \mathbf{0} & \\ & -\omega_1 & \sigma_1 & & & & \\ & & & \ddots & & & \\ & & & & \lambda_k & & \\ & \mathbf{0} & & & & \sigma_s & \omega_s \\ & & & & & -\omega_s & \sigma_s \end{pmatrix}. \tag{13}$$

This form can be obtained using the matrix **P** defined as

$$\mathbf{P} = \begin{pmatrix} \Lambda_1 & \cdots & \Lambda_N \end{pmatrix} \begin{pmatrix} \mathbf{I}_k & & & & \\ & 1 & 1 & & \\ & i & -i & & \\ & & & \ddots & \\ & & & & 1 \quad 1 \\ & & & & i \quad -i \end{pmatrix}^{-1}, \tag{14}$$

where $\Lambda_1, \ldots, \Lambda_N$ are the eigenvectors of matrix **A**. The state-space equations (2) and (3) become

$$\dot{\mathbf{x}}_m = \mathbf{P}^{-1}\mathbf{A}\mathbf{P}\mathbf{x}_\mathbf{m} + \mathbf{P}^{-1}\mathbf{B}\mathbf{u}, \tag{15}$$

$$\mathbf{y}_m = \mathbf{C}\mathbf{P}\mathbf{x}_m + \mathbf{D}\mathbf{u}, \tag{16}$$

and we can define the new matrices $\mathbf{A}_m = \mathbf{P}^{-1}\mathbf{A}\mathbf{P}$, $\mathbf{B}_m = \mathbf{P}^{-1}\mathbf{B}$, $\mathbf{C}_m = \mathbf{C}\mathbf{P}$, $\mathbf{D}_m = \mathbf{D}$. In our case, the outputs $\mathbf{y}_m$ provide the positions/accelerations along the generalized coordinates of the suspension.

C. Kalman filtering

We have now to verify that all the state vector components of the estimated models are observable. This can be done by calculating the observability gramian matrix $\mathcal{O}$ of the system[12]

$$\mathcal{O} = \int_0^\infty e^{\mathbf{A}^T t}\mathbf{C}\mathbf{C}^T e^{\mathbf{A}t} dt. \tag{17}$$

If $\mathcal{O}$ is non singular, a state observer capable of providing outputs proportional to each mode of the system can be implemented.

The most common state estimator used in control theory is the Kalman filter.[13] It is essentially a recursive linear filter based on a predictor-corrector type estimator that is optimal in the sense that it minimizes the estimated error covariance. Assuming the noises **w** and **v** are white and Gaussian distributed with zero mean and covariance matrices **R** and **Q**, the Kalman filter estimates a process by using a form of feedback control: it calculates the process state at some time and then obtains feedback in the form of noisy measurements.

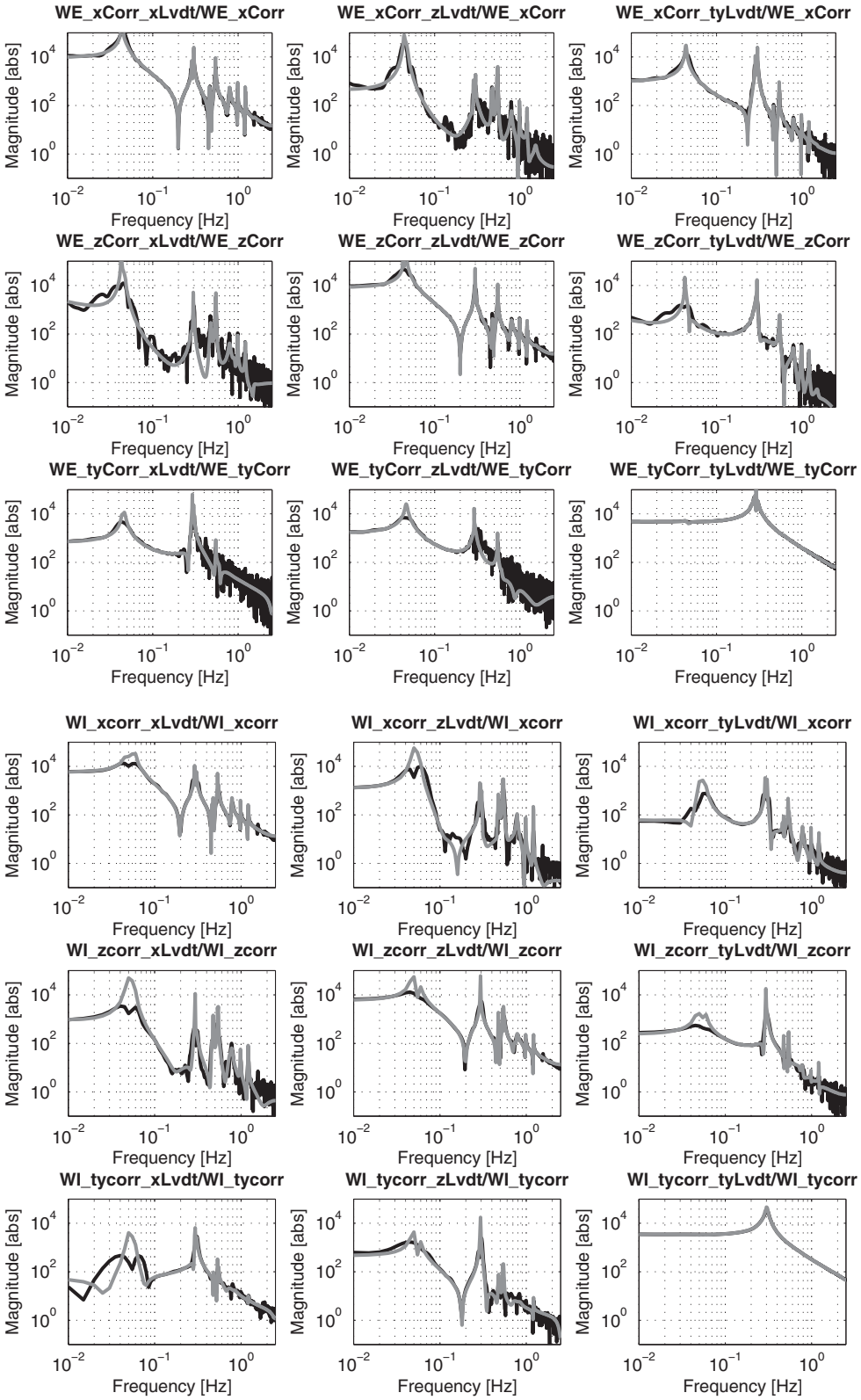

FIG. 3. Comparison between the transfer function matrix obtained from the LVDTs measurements (black curves) and the frequency response of the linear models calculated using subspace system identification (gray curves). The rows represent the excitations (xCorr, zCorr, tyCorr), while the columns are the sensors (xLvdt, zLvdt, tyLvdt). The top 3×3 matrix shows the results obtained with the west end IP, while the bottom matrix is relative to the west input IP.

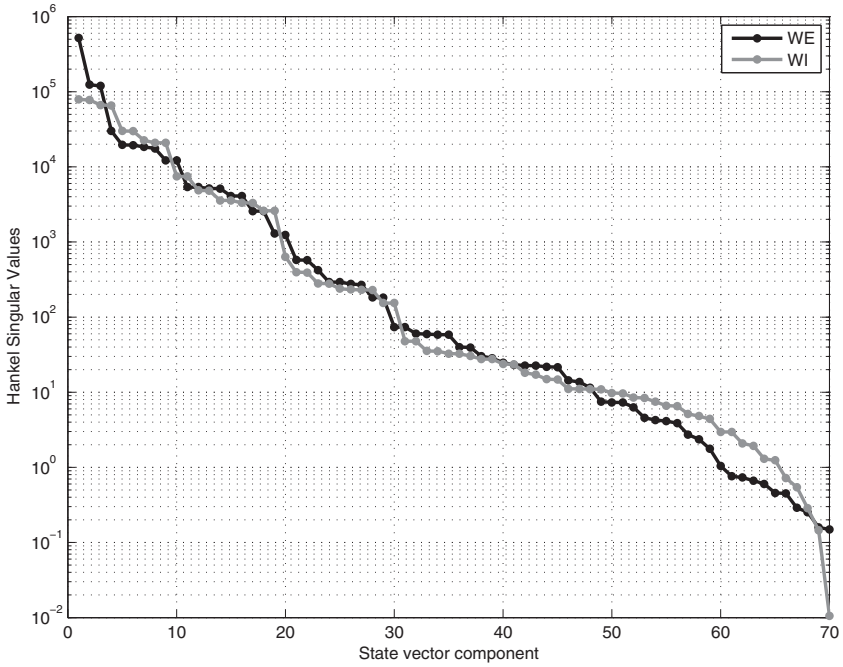

FIG. 4. Hankel singular values of two state-space models of order $N = 70$ calculated from the WE (black points) and the WI (gray points) data.

Using the subspace system identification method it is possible to extract some characteristics of the process and measurement noises **w** and **v**. In particular, we can calculate the matrix **K** that transforms the measurement noise into the process noise, $\mathbf{w} = \mathbf{K}\mathbf{v}$, and the covariance matrix **Q**. Combining **K** and **Q** with the Eqs. (15) and (16), we can rewrite our modal state-space representation in the form

$$\dot{\mathbf{x}}_m = \mathbf{A}_m\mathbf{x}_m + \mathbf{B}_m\mathbf{u} + \mathbf{K}\mathbf{Q}\mathbf{e}(t), \tag{18}$$

$$\mathbf{y}_m = \mathbf{C}_m\mathbf{x}_m + \mathbf{D}_m\mathbf{u} + \mathbf{e}(t), \tag{19}$$

where $\mathbf{e}(t)$ is a normalized noise source. In this way a Kalman state estimator for this system can be obtained simply using identity covariance matrices.

III. EXPERIMENTAL RESULTS

The measurements consisted of three open-loop experiments for each selected SA. We excited the IPs of the west end (WE) and west input (WI) suspensions with band-limited white noise using the three coil-magnet actuators placed on the top ring in succession and we measured the LVDTs and accelerometer signals. In each experiment, we shook for 1800 s and acquired the LVDTs and accelerometer signals with 50 Hz sampling frequency.

We calculated three state-space representations of the LVDT model (Eqs. (9) and (10)) one for each excitation, with order $N = 30$. Therefore, we obtained the estimates $\hat{\mathbf{A}}_L^i$, $\hat{\mathbf{B}}_L^i$, $\hat{\mathbf{C}}_L^i$, $\hat{\mathbf{D}}_L^i$ with $i = 1, 2, 3$, where each $\hat{\mathbf{A}}_L^i$ is 30×30, $\hat{\mathbf{B}}_L^i$ is 30×1, $\hat{\mathbf{C}}_L^i$ is 3×30, and $\hat{\mathbf{D}}_L^i$ is 3×1. The results are shown

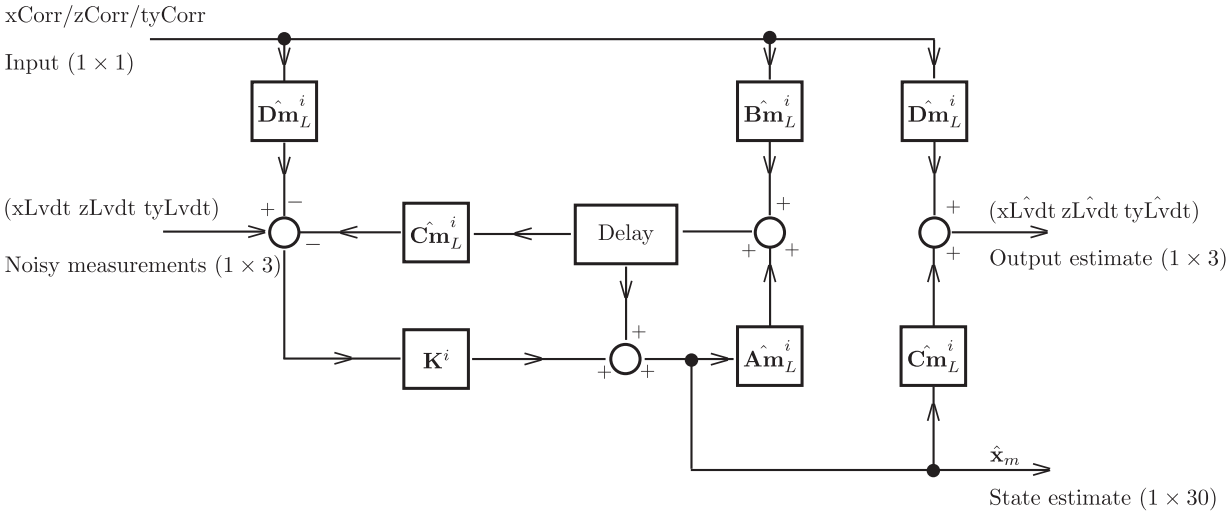

FIG. 5. Block diagram of the three discrete Kalman filters that we have calculated. For each filter the inputs are constituted by the excitation and the measurements, while the outputs are the state and output estimates. $\hat{\mathbf{Am}}_L^i$, $\hat{\mathbf{Bm}}_L^i$, $\hat{\mathbf{Cm}}_L^i$, $\hat{\mathbf{Dm}}_L^i$ with $i = 1, 2, 3$ are the identified state space matrices in modal representation, while $\mathbf{K^i}$ with $i = 1, 2, 3$ are the Kalman gains obtained solving the discrete algebraic Riccati equation (see Ref. 13).

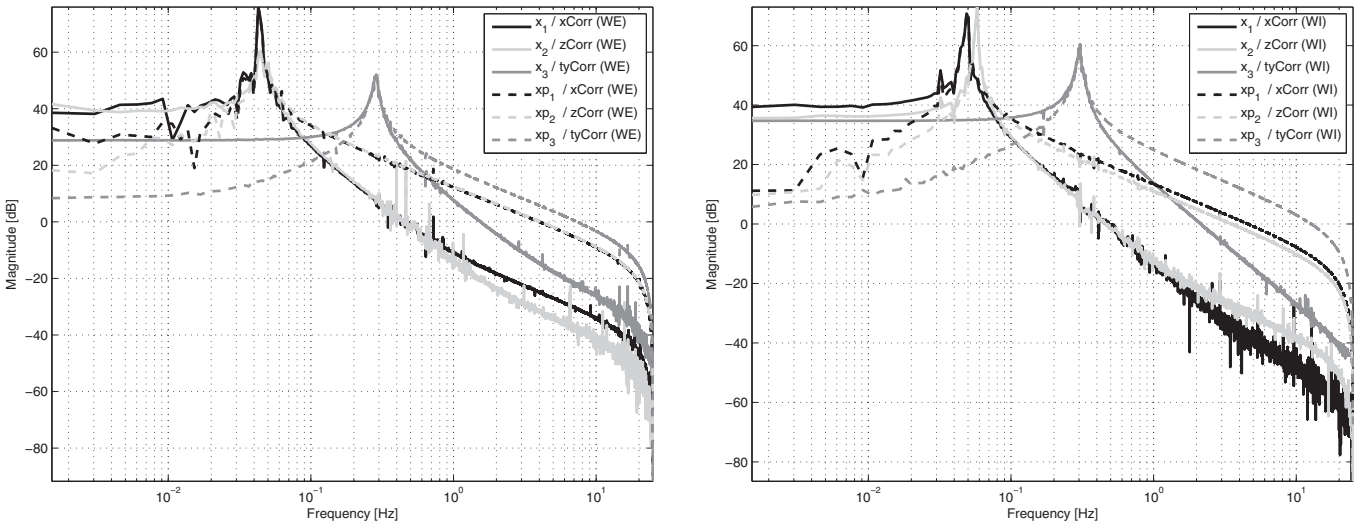

FIG. 6. Transfer functions between the state outputs of the Kalman filters and the relative coil-magnet actuators signals (xCorr, zCorr, tyCorr) for the WE (top) and WI (bottom) suspensions. For clarity only the state vector of the main modes $(x_1, x_2, x_3, \dot{x}_1, \dot{x}_2, \dot{x}_3)$ is shown.

in Fig. 3, where the black curves represent the measured transfer function matrices of the west end (top) and west input (bottom) IPs and the gray curves are the frequency responses of the identified state space models. Even though the quality factors of some modes are overestimated, a good level of agreement is reached.

The value of N has been chosen to have the minimum order that gives an accurate fit of the experimental data over the desired frequency range. Looking at the experimental transfer functions of Fig. 3, we see that, in the band 0.01 Hz $< f <$ 2.5 Hz, there are ~15 resonances in both the WE and WI data. To test this hypothesis, we estimated a high order model for each data set and calculated its Hankel singular values σ_i. These parameters, that are commonly used in control theory for model reduction, provide a measure of the energy of each state components of a linear model.[14] They are defined as the square root of the eigenvalues of the product between the controllability and the observability gramian matrices

$$\sigma_i = \sqrt{\lambda_i(\mathcal{C}\mathcal{O})}, \tag{20}$$

where $\mathcal{C}$ is given by

$$\mathcal{C} = \int_0^\infty e^{\mathbf{A}t}\mathbf{B}\mathbf{B}^T e^{\mathbf{A}^T t}dt. \tag{21}$$

Figure 4 shows the Hankel singular values of a model of order $N = 70$ calculated with WE and WI data. As expected, the last significant drop in the singular values corresponds to ~30 dominant modes in the system.

After applying the procedure described in Subsection II B to the estimated state-space models and verifying their observability, we calculated three discrete Kalman filters, one for each degree of freedom excited (see the block diagram of Fig. 5). Every estimator has 4 inputs, constituted by the excitations (xCorr, zCorr, or tyCorr) and the measurements (xLvdt, zLvdt, and tyLvdt) and 33 outputs, formed by the 30 estimated state vector components ($\hat{\mathbf{x}}_m$) and the 3 estimated outputs (xL$\hat{\text{v}}$dt, zL$\hat{\text{v}}$dt, tyL$\hat{\text{v}}$dt).

In Fig. 6 we show the transfer functions between the state outputs of one observer, relative to the main resonance modes $(x_1, x_2, x_3, \dot{x}_1, \dot{x}_2, \dot{x}_3)$, and its actuator signal input. The geometrical orientation of (x_1, x_2, x_3) is, in general, not aligned with (x, z, θ_y) but depends on random factors such as the asymmetric stiffness of the IP flex joints. The choice of the filter is arbitrary since the coil-magnets are not diagonalized and therefore each of them excites all the modes of the system. Looking at Fig. 6 we can notice that, as expected, the position transfer functions (blue, red, and green curves) have an approximate $1/\omega^2$ high frequency trend, while the velocity transfer functions (magenta, black, and brown curves) tend to zero for low frequencies and goes as $1/\omega$ for high frequencies.

IV. CONCLUSIONS

We successfully applied system identification and Kalman filtering techniques to the Virgo IP mechanical system. A state observer capable to estimate, using time domain data, every resonance mode of the system independently has been developed.

A first possible application would be the implementation of a closed-loop monitoring tool that provides the real-time position and velocity of the Virgo inverted pendulum along its normal modes. In this way any drift in the mechanical characteristics of the IP, due, for example, to environmental noise, can be detected and studied. This work will be the subject of a forthcoming paper.

Kalman filters are commonly used for the development of MIMO optimal dynamic regulators through the linear quadratic Gaussian (LQG) design.[15] Therefore, since a plant state observer is available, we could substitute the classical SISO design approach, currently used in the Virgo IP control, with a multivariable feedback technique such as the LQG. In this way the control diagonalization would no longer be required, and consequently it would be possible to optimize the loop parameters for both the mixed and diagonal term elements of the sensor/actuator transfer function matrix.

[1]T. Accadia, F. Acernese, F. Antonucci, S. Aoudia, K. G. Arun, P. Astone, G. Ballardin, F. Barone, M. Barsuglia, Th. S. Bauer, M. G. Beker, A. Belletoile, S. Bigotta, S. Birindelli, M. A. Bizouard, M. Blom, C. Boccara, F. Bondu, L. Bonelli, R. Bonnand, L. Bosi, S. Braccini, C. Bradaschia, A. Brillet, V. Brisson, R. Budzyński, T. Bulik, H. J. Bulten, D. Buskulic, C. Buy, G. Cagnoli, E. Calloni, E. Campagna, B. Canuel, F. Carbognani, F. Cavalier, R. Cavalieri, G. Cella, E. Cesarini, E. Chassande-Mottin, A. Chincarini, F. Cleva, E. Coccia, C. N. Colacino, J. Colas, A. Colla, M. Colombini, A. Corsi, J.-P. Coulon, E. Cuoco, S. D'Antonio, A. Dari, V. Dattilo, M. Davier, R. Day, R. De Rosa, M. del Prete, L. Di Fiore, A. Di Lieto, M. Di Paolo Emilio, A. Di Virgilio, A. Dietz, M. Drago, V. Fafone, I. Ferrante, F. Fidecaro, I. Fiori, R. Flaminio, J.-D. Fournier, J. Franc, S. Frasca, F. Frasconi, A. Freise, M. Galimberti, L. Gammaitoni, F. Garufi, G. Gemme, E. Genin, A. Gennai, A. Giazotto, R. Gouaty, M. Granata, C. Greverie, G. Guidi, H. Heitmann, P. Hello, S. Hild, D. Huet, P. Jaranowski, I. Kowalska, A. Królak, P. La Penna, N. Leroy, N. Letendre, T. G. F. Li, M. Lorenzini, V. Loriette, G. Losurdo, J.-M. Mackowski, E. Majorana, N. Man, M. Mantovani, F. Marchesoni, F. Marion, J. Marque, F. Martelli, A. Masserot, F. Menzinger, C. Michel, L. Milano, Y. Minenkov, M. Mohan, J. Moreau, N. Morgado, A. Morgia, S. Mosca, V. Moscatelli, B. Mours, I. Neri, F. Nocera, G. Pagliaroli, C. Palomba, F. Paoletti, S. Pardi, M. Parisi, A. Pasqualetti, R. Passaquieti, D. Passuello, G. Persichetti, M. Pichot, F. Piergiovanni, M. Pietka, L. Pinard, R. Poggiani, M. Prato, G. A. Prodi, M. Punturo, P. Puppo, O. Rabaste, D. S. Rabeling, P. Rapagnani, V. Re, T. Regimbau, F. Ricci, F. Robinet, A. Rocchi, L. Rolland, R. Romano, D. Rosińska, P. Ruggi, B. Sassolas, D. Sentenac, R. Sturani, B. Swinkels, A. Toncelli, M. Tonelli, E. Tournefier, F. Travasso, J. Trummer, G. Vajente, J. F. J. van den Brand, S. van der Putten, M. Vavoulidis, G. Vedovato, D. Verkindt, F. Vetrano, A. Viceré, J.-Y. Vinet, H. Vocca, M. Was, and M. Yvert, J. Phys.: Conf. Ser. **203**(1), 012074 (2010).

[2]B. P. Abbott, R. Abbott, R. Adhikari, P. Ajith, B. Allen, G. Allen, R. S. Amin, S. B. Anderson, W. G. Anderson, M. A. Arain, M. Araya, H. Armandula, P. Armor, Y. Aso, S. Aston, P. Aufmuth, C. Aulbert, S. Babak, P. Baker, S. Ballmer, C. Barker, D. Barker, B. Barr, P. Barriga, L. Barsotti, M. A. Barton, I. Bartos, R. Bassiri, M. Bastarrika, B. Behnke, M. Benacquista, J. Betzwieser, P. T. Beyersdorf, I. A. Bilenko, G. Billingsley, R. Biswas, E. Black, J. K. Blackburn, L. Blackburn, D. Blair, B. Bland, T. P. Bodiya, L. Bogue, R. Bork, V. Boschi, S. Bose, P. R. Brady, V. B. Braginsky, J. E. Brau, D. O. Bridges, M. Brinkmann, A. F. Brooks, D. A. Brown, A. Brummit, G. Brunet, A. Bullington, A. Buonanno, O. Burmeister, R. L. Byer, L. Cadonati, J. B. Camp, J. Cannizzo, K. C. Cannon, J. Cao, L. Cardenas, S. Caride, G. Castaldi, S. Caudill, M. Cavaglià, C. Cepeda, T. Chalermsongsak, E. Chalkley, P. Charlton, S. Chatterji, S. Chelkowski, Y. Chen, N. Christensen, C. T. Y. Chung, D. Clark, J. Clark, J. H. Clayton, T. Cokelaer, C. N. Colacino, R. Conte, D. Cook, T. R. C. Corbitt, N. Cornish, D. Coward, D. C. Coyne, J. D. E. Creighton, T. D. Creighton, A. M. Cruise, R. M. Culter, A. Cumming, L. Cunningham, S. L. Danilishin, K. Danzmann, B. Daudert, G. Davies, E. J. Daw, D. DeBra, J. Degallaix, V. Dergachev, S. Desai, R. DeSalvo, S. Dhurandhar, M. DÃ-az, A. Dietz, F. Donovan, K. L. Dooley, E. E. Doomes, R. W. P. Drever, J. Dueck, I. Duke, J.-C. Dumas, J. G. Dwyer, C. Echols, M. Edgar, A. Effler, P. Ehrens, E. Espinoza, T. Etzel, M. Evans, T. Evans, S. Fairhurst, Y. Faltas, Y. Fan, D. Fazi, H. Fehrmenn, L. S. Finn, K. Flasch, S. Foley, C. Forrest, N. Fotopoulos, A. Franzen, M. Frede, M. Frei, Z. Frei, A. Freise, R. Frey, T. Fricke, P. Fritschel, V. V. Frolov, M. Fyffe, V. Galdi, J. A. Garofoli, I. Gholami, J. A. Giaime, S. Giampanis, K. D. Giardina, K. Goda, E. Goetz, L. M. Goggin, G. González, M. L. Gorodetsky, S. Goßler, R. Gouaty, A. Grant, S. Gras, C. Gray, M. Gray, R. J. S. Greenhalgh, A. M. Gretarsson, F. Grimaldi, R. Grosso, H. Grote, S. Grunewald, M. Guenther, E. K. Gustafson, R. Gustafson, B. Hage, J. M. Hallam, D. Hammer, G. D. Hammond, C. Hanna, J. Hanson, J. Harms, G. M. Harry, I. W. Harry, E. D. Harstad, K. Haughian, K. Hayama, J. Heefner, I. S. Heng, A. Heptonstall, M. Hewitson, S. Hild, E. Hirose, D. Hoak, K. A. Hodge, K. Holt, D. J. Hosken, J. Hough, D. Hoyland, B. Hughey, S. H. Huttner, D. R. Ingram, T. Isogai, M. Ito, A. Ivanov, B. Johnson, W. W. Johnson, D. I. Jones, G. Jones, R. Jones, L. Ju, P. Kalmus, V. Kalogera, S. Kandhasamy, J. Kanner, D. Kasprzyk, E. Katsavounidis, K. Kawabe, S. Kawamura, F. Kawazoe, W. Kells, D. G. Keppel, A. Khalaidovski, F. Y. Khalili, R. Khan, E. Khazanov, P. King, J. S. Kissel, S. Klimenko, K. Kokeyama, V. Kondrashov, R. Kopparapu, S. Koranda, D. Kozak, B. Krishnan, R. Kumar, P. Kwee, P. K. Lam, M. Landry, B. Lantz, A. Lazzarini, H. Lei, M. Lei, N. Leindecker, I. Leonor, C. Li, H. Lin, P. E. Lindquist, T. B. Littenberg, N. A. Lockerbie, D. Lodhia, M. Longo, M. Lormand, P. Lu, M. Lubinski, A. Lucianetti, H. Lück, B. Machenschalk, M. MacInnis, M. Mageswaran, K. Mailand, I. Mandel, V. Mandic, S. Márka, Z. Márka, A. Markosyan, J. Markowitz, E. Maros, I. W. Martin, R. M. Martin, J. N. Marx, K. Mason, F. Matichard, L. Matone, R. A. Matzner, N. Mavalvala, R. McCarthy, D. E. McClelland, S. C. McGuire, M. McHugh, G. McIntyre, D. J. A. McKechan, K. McKenzie, M. Mehmet, A. Melatos, A. C. Melissinos, D. F. Menéndez, G. Mendell, R. A. Mercer, S. Meshkov, C. Messenger, M. S. Meyer, J. Miller, J. Minelli, Y. Mino, V. P. Mitrofanov, G. Mitselmakher, R. Mittleman, O. Miyakawa, B. Moe, S. D. Mohanty, S. R. P. Mohapatra, G. Moreno, T. Morioka, K. Mors, K. Mossavi, C. MowLowry, G. Mueller, H. Müller-Ebhardt, D. Muhammad, S. Mukherjee, H. Mukhopadhyay, A. Mullavey, J. Munch, P. G. Murray, E. Myers, J. Myers, T. Nash, J. Nelson, G. Newton, A. Nishizawa, K. Numata, J. O'Dell, B. O'Reilly, R. O'Shaughnessy, E. Ochsner, G. H. Ogin, D. J. Ottaway, R. S. Ottens, H. Overmier, B. J. Owen, Y. Pan, C. Pankow, M. A. Papa, V. Parameshwaraiah, P. Patel, M. Pedraza, S. Penn, A. Perraca, V. Pierro, I. M. Pinto, M. Pitkin, H. J. Pletsch, M. V. Plissi, F. Postiglione, M. Principe, R. Prix, L. Prokhorov, O. Punken, V. Quetschke, F. J. Raab, D. S. Rabeling, H. Radkins, P. Raffai, Z. Raics, N. Rainer, M. Rakhmanov, V. Raymond, C. M. Reed, T. Reed, H. Rehbein, S. Reid, D. H. Reitze, R. Riesen, K. Riles, B. Rivera, P. Roberts, N. A. Robertson, C. Robinson, E. L. Robinson, S. Roddy, C. Rver, J. Rollins, J. D. Romano, J. H. Romie, S. Rowan, A. Rüdiger, P. Russell, K. Ryan, S. Sakata, L. Sancho de la Jordana, V. Sandberg, V. Sannibale, L. SantamarÃ-a, S. Saraf, P. Sarin, B. S. Sathyaprakash, S. Sato, M. Satterthwaite, P. R. Saulson, R. Savage, P. Savov, M. Scanlan, R. Schilling, R. Schnabel, R. Schofield, B. Schulz, B. F. Schutz, P. Schwinberg, J. Scott, S. M. Scott, A. C. Searle, B. Sears, F. Seifert, D. Sellers, A. S. Sengupta, A. Sergeev, B. Shapiro, P. Shawhan, D. H. Shoemaker, A. Sibley, X. Siemens, D. Sigg, S. Sinha, A. M. Sintes, B. J. J. Slagmolen, J. Slutsky, J. R. Smith, M. R. Smith, N. D. Smith, K. Somiya, B. Sorazu, A. Stein, L. C. Stein, S. Steplewski, A. Stochino, R. Stone, K. A. Strain, S. Strigin, A. Stroeer, A. L. Stuver, T. Z. Summerscales, K.-X. Sun, M. Sung, P. J. Sutton, G. P. Szokoly, D. Talukder, L. Tang, D. B. Tanner, S. P. Tarabrin, J. R. Taylor, R. Taylor, J. Thacker, K. A. Thorne, A. Thüring, K. V. Tokmakov, C. Torres, C. Torrie, G. Traylor, M. Trias, D. Ugolini, J. Ulmen, K. Urbanek, H. Vahlbruch, M. Vallisneri, C. Van Den Broeck, M. V. van der Sluys, A. A. van Veggel, S. Vass, R. Vaulin, A. Vecchio, J. Veitch, P. Veitch, C. Veltkamp, A. Villar, C. Vorvick, S. P. Vyachanin, S. J. Waldman, L. Wallace, R. L. Ward, A. Weidner, M. Weinert, A. J. Weinstein, R. Weiss, L. Wen, S. Wen, K. Wette, J. T. Whelan, S. E. Whitcomb, B. F. Whiting, C. Wilkinson, P. A. Willems, H. R. Williams, L. Williams, B. Willke, I. Wilmut, L. Winkelmann, W. Winkler, C. C. Wipf, A. G. Wiseman, G. Woan, R. Wooley, J. Worden, W. Wu, I. Yakushin, H. Yamamoto, Z. Yan, S. Yoshida, M. Zanolin, J. Zhang, L. Zhang, C. Zhao, N. Zotov, M. E. Zucker, H. zur Mühlen, and J. Zweizig, Rep. Prog. Phys. **72**(7), 076901 (2009).

[3]F. Acernese, M. Alshourbagy, F. Antonucci, S. Aoudia, K. G. Arun, P. Astone, G. Ballardin, F. Barone, M. Barsuglia, Th. S. Bauer, M. G. Beker, S. Bigotta, S. Birindelli, M. A. Bizouard, C. Boccara, F. Bondu, L. Bonelli, L. Bosi, S. Braccini, C. Bradaschia, A. Brillet, V. Brisson, H. J. Bulten, D. Buskulic, G. Cagnoli, E. Calloni, E. Campagna, B. Canuel, F. Carbognani, F. Cavalier, R. Cavalieri, G. Cella, E. Cesarini, E. Chassande-Mottin, S. Chatterji, A. Chincarini, F. Cleva, E. Coccia, P. F. Cohadon, J. Colas, M. Colombini, C. Corda, A. Corsi, J.-P. Coulon, E. Cuoco, S. D'Antonio, A. Dari, V. Dattilo, M. Davier, R. Day, R. De Rosa, M. del Prete, L. Di Fiore, A. Di Lieto, M. Di Paolo Emilio, A. Di Virgilio, M. Drago, V. Fafone, I. Ferrante, F. Fidecaro, I. Fiori, R. Flaminio, J.-D. Fournier, J. Franc, S. Frasca, F. Frasconi, A. Freise, L. Gammaitoni, F. Garufi, G. Gemme, E. Genin, A. Gennai, A. Giazotto, M. Granata, V. Granata, C. Greverie, G. M. Guidi, A. Heidmann, H. Heitmann, P. Hello, S. Hild, D. Huet, P. La Penna, M. Laval, N. Leroy, N. Letendre, M. Lorenzini, V. Loriette, G. Losurdo, J. M. Mackowski, E. Majorana, N. Man, M. Mantovani, F. Marchesoni, F. Marion, J. Marque, F. Martelli, A. Masserot, F. Menzinger, C. Michel, L. Milano, Y. Minenkov, M. Mohan, J. Moreau, N. Morgado, A. Morgia, S. Mosca, B. Mours, I. Neri, F. Nocera, G. Pagliaroli, C. Palomba, F. Paoletti, S. Pardi, A. Pasqualetti, R. Passaquieti, D. Passuello, G. Persichetti, F. Piergiovanni, L. Pinard, R. Poggiani, G. A. Prodi, M. Punturo, P. Puppo, O. Rabaste, P. Rapagnani, V. Re, T. Regimbau, F. Ricci, F. Robi-

net, A. Rocchi, L. Rolland, R. Romano, P. Ruggi, F. Salemi, B. Sassolas, D. Sentenac, R. Sturani, B. Swinkels, R. Terenzi, A. Toncelli, M. Tonelli, E. Tournefier, F. Travasso, J. Trummer, G. Vajente, J. F. J. van den Brand, S. van der Putten, M. Vavoulidis, G. Vedovato, D. Verkindt, F. Vetrano, A. Viceré, J.-Y. Vinet, H. Vocca, M. Was, and M. Yvert, Technical note VIR-0027A-09, Virgo, 2009.

[4]Advanced LIGO Team, Technical note LIGO-M060056-v2, LIGO, 2006.

[5]F. Acernese, F. Antonucci, S. Aoudia, K. G. Arun, P. Astone, G. Ballardin, F. Barone, M. Barsuglia, Th. S. Bauer, M. G. Beker, S. Bigotta, S. Birindelli, M. Bitossi, M. A. Bizouard, M. Blom, C. Boccara, F. Bondu, L. Bonelli, L. Bosi, S. Braccini, C. Bradaschia, A. Brillet, V. Brisson, R. Budzyński, T. Bulik, H. J. Bulten, D. Buskulic, G. Cagnoli, E. Calloni, E. Campagna, B. Canuel, F. Carbognani, F. Cavalier, R. Cavalieri, G. Cella, E. Cesarini, E. Chassande-Mottin, A. Chincarini, F. Cleva, E. Coccia, C. N. Colacino, J. Colas, A. Colla, M. Colombini, C. Corda, A. Corsi, J.-P. Coulon, E. Cuoco, S. D'Antonio, A. Dari, V. Dattilo, M. Davier, R. Day, R. De Rosa, M. Del Prete, L. Di Fiore, A. Di Lieto, M. Di Paolo Emilio, A. Di Virgilio, A. Dietz, M. Drago, V. Fafone, I. Ferrante, F. Fidecaro, I. Fiori, R. Flaminio, J.-D. Fournier, J. Franc, S. Frasca, F. Frasconi, A. Freise, L. Gammaitoni, F. Garufi, G. Gemme, E. Genin, A. Gennai, A. Giazotto, M. Granata, C. Greverie, G. Guidi, H. Heitmann, P. Hello, S. Hild, D. Huet, P. Jaranowski, I. Kowalska, A. Królak, P. La Penna, N. Leroy, N. Letendre, T. G. F. Li, M. Lorenzini, V. Loriette, G. Losurdo, J.-M. Mackowski, E. Majorana, N. Man, M. Mantovani, F. Marchesoni, F. Marion, J. Marque, F. Martelli, A. Masserot, F. Menzinger, C. Michel, L. Milano, Y. Minenkov, M. Mohan, J. Moreau, N. Morgado, A. Morgia, S. Mosca, V. Moscatelli, B. Mours, I. Neri, F. Nocera, G. Pagliaroli, C. Palomba, F. Paoletti, S. Pardi, M. Parisi, A. Pasqualetti, R. Passaquieti, D. Passuello, G. Persichetti, M. Pichot, F. Piergiovanni, M. Pietka, L. Pinard, R. Poggiani, M. Prato, G. A. Prodi, M. Punturo, P. Puppo, O. Rabaste, D. S. Rabeling, P. Rapagnani, V. Re, T. Regimbau, F. Ricci, F. Robinet, A. Rocchi, L. Rolland, R. Romano, D. Rosińska, P. Ruggi, F. Salemi, B. Sassolas, D. Sentenac, R. Sturani, B. Swinkels, A. Toncelli, M. Tonelli, E. Tournefier, F. Travasso, J. Trummer, G. Vajente, J. F. J. van den Brand, S. van der Putten, M. Vavoulidis, G. Vedovato, D. Verkindt, F. Vetrano, A. Viceré, J.-Y. Vinet, H. Vocca, M. Was, and M. Yvert, Astropart. Phys. **33**(3), 182 (2010).

[6]G. Losurdo, M. Bernardini, S. Braccini, C. Bradaschia, C. Casciano, V. Dattilo, R. De Salvo, A. Di Virgilio, F. Frasconi, A. Gaddi, A. Gennai, A. Giazotto, H. B. Pan, F. Paoletti, A. Pasqualetti, R. Passaquieti, D. Passuello, R. Taddei, Z. Zhang, G. Cella, E. Cuoco, E. D'Ambrosio, F. Fidecaro, S. Gaggero, P. La Penna, S. Mancini, R. Poggiani, A. Viceré, M. Mazzoni, R. Stanga, L. Holloway, and J. Winterflood, Rev. Sci. Instrum. **70**(5), 2507 (1999).

[7]L. Meirovitch, *Fundamentals of Vibrations* (McGraw-Hill, New York, 2001).

[8]A. Gennai, T. Maiani, S. Mancini, D. Passuello, and R. Taddei, Technical note VIR-NOT-PIS-4900-102, Virgo, 1997.

[9]L. Ljung, *System Identification: Theory for the User* (Prentice-Hall, Upper Saddle River, NJ, 1999).

[10]P. Van Overschee and B. De Moor, Automatica **30**(1), 75 (1994), Special issue on statistical signal processing and control.

[11]Even though the VIRGO IP is designed to be symmetric, unavoidable small mechanical asymmetries makes its modes non degenerate.

[12]T. Kailath, *Linear Systems* (Prentice-Hall, Englewood Cliffs, NJ, 1980).

[13]A. P. Andrews and M. S. Grewal, *Kalman Filtering: Theory and Practice Using matlab* (Wiley, New York, 2001).

[14]A. C. Antoulas, *Approximation of large-scale dynamical systems* (SIAM, Philadelphia, PA, 2005).

[15]J. M. Maciejowski, *Multivariable Feedback Design* (Addison-Wesley, Wokingham, UK, 1989).